Proceedings of the *SPIE Defense, Security + Sensing;*
Conference DS209: Head- and Helmet-Mounted Displays XVI: Design and Applications. Orlando, FL, April 25-29, 2011

Transfer Alignment from a Personal Locator System to a Handheld or Head-mounted Instrument

Lauro Ojeda and Johann Borenstein
University of Michigan, Ann Arbor, MI 48109

ABSTRACT

This paper presents a method for computing position and attitude of an instrument attached to the human body such as a handheld or head-mounted video camera. The system uses two Inertial Measurement Units (IMUs). One IMU is part of our earlier-developed Personal Dead-Reckoning (PDR) system, which tracks the position and heading of a walking person relative to a known starting position. The other IMU is rigidly attached to the handheld or head-mounted instrument.

Our existing PDR system is substantially more accurate than conventional IMU-based systems because the IMU is mounted on the foot of the user where error correction techniques can be applied that are unavailable for IMUs mounted anywhere else on the body. However, if the walker is waving a handheld or head-mounted instrument, the position and attitude of the instrument is not known. Equipping the instrument with an additional IMU is by itself an unsatisfactory solution because that IMU is subject to accelerometer and gyro drift, which, unlike in the case of the foot-mounted IMU, cannot be corrected and cause unbounded position and heading errors. Our approach uses transfer alignment techniques and takes advantage of the fact that the handheld IMU moves with the walker. This constraint is used to bound and correct errors by a Kalman filter. The paper explains our method and presents extensive experimental results. The results show up to a five-fold reduction in heading errors for the handheld IMU.

Keywords

Transfer alignment, inertial navigation, Kalman filters, personal localization, position estimation, motion capture, head-mounted, helmet-mounted

INTRODUCTION

Some applications require the tracking of position and attitude of an instrument or device attached to the human body, for example, a handheld or head-mounted video camera or display. Reliable solutions for this problem are limited to constrained environments that have been equipped with external devices. By analyzing images from multiple cameras, some systems can track active markers [1], passive markers [2], or even the human limbs [3][4]. Other systems use active signal sources such as magnetic fields [5], electric field sensors [6], radio frequency [7] or sonar [8]. Even though some of these approaches can provide very accurate tracking, all of them have the same limitation: they are limited to lab-style setups that are not practical or possible for many applications.

For everyday uncontrolled environments, a partial solution for this problem exists in the form of motion capture systems. The most common approach uses a constellation of Inertial Measurement Units (IMUs) distributed on the body and estimates each limb location using articulated body models [9][10]. A system presented in [11] combines inertial sensors and sonar to track the body. In these cases the solution of localizing a body part is given as a relative position and attitude with respect to the other parts of the body.

A solution that addresses the problem of localization has been presented in [12]. This work combines GPS for global localization and a helmet mounted IMU for tracking the head. Because of the use of GPS, however, this solution is limited to outdoor applications. A survey of tracking technology can be found in [13] and [14].

This paper presents a method for computing position and attitude of an IMU that is attached to the human body and works in any environment. Our solution uses location updates from our previously developed Personal Dead-reckoning system (PDR) [15] to bound and correct positioning and attitude errors of a body-mounted IMU. For practical purposes we developed our approach and tested it extensively with a handheld IMU. This is the most general and hardest case because the human arm and hand have many degrees of freedom. Our reasoning is that if our solution performs well for this case, it will also work well in simpler cases, such as head or helmet mounted devices. For simplicity, we will refer to all body-mounted IMU as "handheld," keeping in mind that the same solution will work for easier cases, such as head-mounted IMUs.

We present results showing the performance of our system with two types of handheld IMUs, a high-grade and a low-grade one.

THE TRANSFER ALIGNMENT FORMULATION

Our approach for tracking the handheld IMU presents two challenges: pose estimation for the walking person and relative pose estimation for the handheld IMU. The first challenge is met by our earlier-developed PDR system that uses a foot-mounted IMU to track the position and heading of a walking person inside buildings [15]. Because of the mounting location of the IMU in the heel of the user's boot (see Figure 1), the PDR system can apply the Zero Velocity Update (ZUPT) method to correct accelerometer drift. In addition, by exploiting the rectilinear features of the large majority of all buildings, the PDR system provides zero heading errors at steady state in walks of unlimited duration, as explained in [16]. However, the second challenge is harder to meet because the attitude and position of the instrument can change arbitrarily. Just adding an additional IMU provides dissatisfactory results because that IMU is subject to accelerometer and gyro drift, which grow into unbounded position and heading errors that cannot be corrected by the same method that works for the foot-mounted IMU.

Figure 1: The PDR system uses an IMU mounted inside the heel of the user's boot. Other mounting options exist but are not shown here.

In order to reduce the effects of drift and other errors in the handheld IMU, we adopted a method known as Transfer Alignment (TA). TA has been widely used in military applications and in particular in aerospace applications [17][18]. TA works by exploiting the fact that in two loosely connected bodies (i.e., a non-rigid body such as the hand of a person and the person's trunk) some relationship between the parts exist. For this particular application, TA takes advantage of the fact that the X-Y position of the handheld IMU will always be near the X-Y position of the foot and ultimately follows the same path. Our TA formulation uses the accurate position updates from the PDR system to bound and correct position and heading errors of the handheld IMU. The TA error correction for attitude and position is performed by a Kalman filter (KF).

The KF Formulation

Although our main interest was to reduce the heading errors of the handheld IMU, our solution is capable of bounding positioning errors as well, that is because in the KF formulation, attitude and position errors are related. In this paper we will only focus on the analyzing the heading correction problem only.

The KF was designed to model the most significant errors that affect the handheld IMU. Since our main interest was solving the heading alignment problem, the solution was formulated in the X-Y plane. The handheld IMU heading is assumed to be affected by a drift component and white noise:

$$\psi_S = \psi + b_\psi + w \tag{1}$$

Where:

ψ_S – Handheld IMU heading computed from direct gyroscope sensor data integration

b_ψ – Drift component.

ψ – Unknown true heading of the handheld IMU.

w – A generic term to represent the process white noise (i.e. sensor noise).

In some equations w should be interpreted as a vector of uncorrelated white noise components.

The system internally computes attitude using gyroscope information, and uses the tilt components (ϕ, θ) to remove the gravity component from the body accelerations. The resulting gravity-free body accelerations (A_{BX}, A_{BY}) are then used to estimate the acceleration referenced with respect to the navigation frame as follows:

$$\begin{aligned} \ddot{X} &= A_{BX}\cos(\psi_c) - A_{BY}\sin(\psi_c) \\ \ddot{Y} &= A_{BX}\sin(\psi_c) + A_{BX}\cos(\psi_c) \end{aligned} \tag{2}$$

Where:

$\ddot{X}, \ddot{Y}$ – Handheld IMU accelerations referenced with respect to the navigation frame.

In practice, the body accelerations measured by the handheld IMU will have errors. Our system models the body acceleration errors to be affected by a bias drift and a noise component, as follows:

$$\begin{aligned} A_{BX} &= A_X + b_X + w \\ A_{BY} &= A_Y + b_Y + w \end{aligned} \tag{3}$$

Where:

A_X, A_Y – True but unknown body accelerations after removing the gravity component.

b_X, b_Y – Body acceleration bias.

We define the following states for the KF:

$$x' = \begin{bmatrix} X & \dot{X} & b_X & Y & \dot{Y} & b_Y & b_\psi \end{bmatrix} \tag{4}$$

Where:

$\dot{X}, \dot{Y}$ – Handheld IMU velocities referenced with respect to the navigation frame.

X, Y – Handheld IMU positions referenced with respect to the navigation frame.

Using the previously described relations, we define the following state-space formulation:

$$\dot{x} = f(x)x + g(x)u + w$$

$$\begin{bmatrix} \dot{X} \\ \ddot{X} \\ \dot{b}_X \\ \dot{Y} \\ \ddot{Y} \\ \dot{b}_Y \\ \dot{b}_\psi \end{bmatrix} = \begin{bmatrix} 0 & 1 & 0 & 0 & 0 & 0 & 0 \\ 0 & 0 & \cos(\psi + b_\psi) & 0 & 0 & -\sin(\psi + b_\psi) & 0 \\ 0 & 0 & 0 & 0 & 0 & 0 & 0 \\ 0 & 0 & 0 & 0 & 1 & 0 & 0 \\ 0 & 0 & \sin(\psi + b_\psi) & 0 & 0 & \cos(\psi + b_\psi) & 0 \\ 0 & 0 & 0 & 0 & 0 & 0 & 0 \\ 0 & 0 & 0 & 0 & 0 & 0 & 0 \end{bmatrix} \begin{bmatrix} X \\ \dot{X} \\ b_X \\ Y \\ \dot{Y} \\ b_Y \\ b_\psi \end{bmatrix} +$$

$$\begin{bmatrix} 0 & 0 & 0 & 0 & 0 \\ \cos(\psi + b_\psi) & 0 & -\sin(\psi + b_\psi) & 0 & 0 \\ 0 & 1 & 0 & 0 & 0 \\ 0 & 0 & 0 & 0 & 0 \\ \sin(\psi + b_\psi) & 0 & \cos(\psi + b_\psi) & 0 & 0 \\ 0 & 0 & 0 & 1 & 0 \\ 0 & 0 & 0 & 0 & 1 \end{bmatrix} \begin{bmatrix} A_X \\ 0 \\ A_Y \\ 0 \\ 0 \end{bmatrix} + w \qquad (5)$$

As we mentioned before, our method uses the fact that since the two IMUs are connected through the user's body, both will follow approximately the user's trajectory while walking. From the KF formulation, we can say that at any given time the handheld IMU's location is the same as that of the walker but corrupted by noise:

$$\begin{aligned} X_{PDR} &= X + v \\ Y_{PDR} &= Y + v \end{aligned} \qquad (6)$$

where

X_{PDR}, Y_{PDR} – Walker's position estimated by the PDR system.

v – A generic variable used to represent the measurement white noise, which is the expected difference between the PDR and the handheld location.

The positions estimated by the PDR system (X_{PDR}, Y_{PDR}) are used as the KF measurement update. The PDR positioning output can be expressed as a function of the KF states as follows:

$$\begin{bmatrix} X_{PDR} \\ Y_{PDR} \end{bmatrix} = \begin{bmatrix} 1 & 0 & 0 & 0 & 0 & 0 & 0 \\ 0 & 0 & 0 & 1 & 0 & 0 & 0 \end{bmatrix} \begin{bmatrix} X \\ \dot{X} \\ b_X \\ Y \\ \dot{Y} \\ b_Y \\ b_\psi \end{bmatrix} + v \qquad (7)$$

Since our KF computes position X and Y as part of the states, it must be updated continuously as new accelerometer data becomes available. However, since the PDR output has the lowest uncertainty on every footfall, we only update the measurements on footfalls.

Because of the non-linear nature of our KF, we implemented an Extended KF. The error propagation and gain estimation is determined using the Jacobian of the transfer functions:

$$F_L = \frac{\partial(f(x)x + g(x)u)}{\partial x} \quad (8)$$

The KF configurations presented is a feed-forward configuration since the error states are only used to correct the final state, while the system remains un-aware of these errors.

It can be seen in the state-space formulation that the accelerometer error makes no distinction between accelerometer bias and errors resulting from tilt. We found that after prolonged periods of time, the accumulation of gyro errors in the handheld-IMU can eventually introduce significant tilt errors. Under these conditions, the filter may fail to predict the states correctly. For example, the tilt error changes signs (goes from positive to negative value and vice versa) when the user turns 180°. Therefore, if the tilt error is large, the KF could take a long time to reach steady state. This effect is more noticeable when the user changes direction of travel, Figure 2 shows large positioning errors immediately after every sharp turn, caused by tilt errors.

The Feedback KF Formulation

The solution for the adverse effects of tilt angle errors is to include them in the KF estimate and feed them back into the system; this is known as a feedback KF configuration. One way to do so is by increasing the number of states in the KF to include tilt errors. Alternatively a separate KF that deals with the tilt errors only could be used. We opted for the latter solution as it requires less computational resources. We defined an indirect KF with the following states:

$$x' = \begin{bmatrix} \phi_e & \theta_e \end{bmatrix} \quad (9)$$

Where:

ϕ_e, θ_e – Roll and pitch errors

We modeled the tilt errors as constants affected by white noise:

$$\dot{x} = \begin{bmatrix} \dot{\phi}_e \\ \dot{\theta}_e \end{bmatrix} = \begin{bmatrix} 0 & 0 \\ 0 & 0 \end{bmatrix} \begin{bmatrix} \phi_e \\ \theta_e \end{bmatrix} + w$$

Without additional information, it is not possible to separate the tilt and drift errors. However, because of the random nature of drift, it is safe to say that the low frequency component of the estimated drift used in the feed-forward KF formulation is more likely to be caused by tilt errors. Therefore, we can use some of the states estimated by the original KF as input measurements for the KF that estimates tilt errors. For small tilt errors, the following approximations can be used:

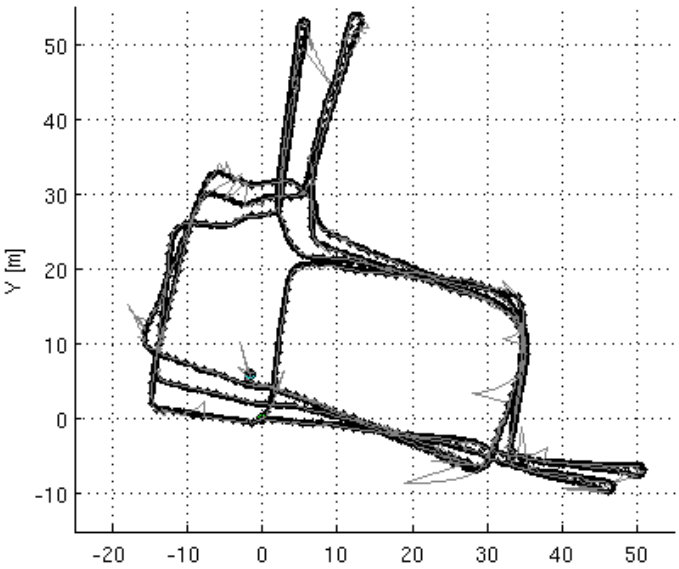

Figure 2: Walker's trajectory as recorded by: (thick dark line) PDR system output, and (thin gray line) feed-forward KF solution applied to the handheld IMU.

$$\theta_e = \frac{b_X}{g} + v$$
$$\phi_e = -\frac{b_Y}{g} + v \tag{11}$$

Where:

g – Gravity acceleration constant

The linear connection between the input measurements and the state vector is:

$$\begin{bmatrix} b_Y \\ b_x \end{bmatrix} = \begin{bmatrix} g & 0 \\ 0 & -g \end{bmatrix} \begin{bmatrix} \phi_e \\ \theta_e \end{bmatrix} + v \tag{12}$$

As the result of this implementation, we were able to reduce significantly the effects of tilt errors as shown in Figure 3, which shows the result of applying the two stage KF formulation over the same data set shown in Figure 2.

KF Parameter Tuning

The measurement covariance errors (position X and Y) are determined based on the expected variance of the handheld IMU location relative to the foot-mounted IMU. The measurement covariance is not dependent on the handheld IMU and can be estimated or guessed with relative accuracy. Since we can expect these parameters to vary for different IMU handling conditions, these parameters should vary accordingly for higher accuracy. In our system we assumed that the covariance errors are constant and time-invariant, we also assume that both axes have similar covariance errors (X ≈ Y error covariance). Since we used the same PDR configuration for all the experiments, we only needed to determine a single covariance error value for all of the experiments shown later.

The process covariance errors are related to the intrinsic sensor errors such as bias, effects of temperature, acceleration sensitivity, etc. In theory, the KF could be designed to work with all the individual error components. In practice, however, there is a tradeoff between system accuracy and filter complexity. Our system treats the combination of several sources of errors as unified random noise, therefore the process variance noise was determined experimentally by trial and error. The filter uses five covariance error values: X and Y accelerometer bias, X and Y accelerometer noise level, and heading error. We assumed that the X and Y covariance errors were similar, therefore we only needed to tune three parameters. As can be expected, these parameters will be different for different handheld IMUs. Since in our experiments we used two handheld IMUs, we used one set of parameters for each one.

For the feedback KF configuration that uses a second KF for bounding tilt errors, it is safe to assume that the roll and tilt covariance errors are similar. Therefore during the KF tuning, we only needed to estimate one measurement error and one process error. Both types of errors (process and measurement) will be dependent on the quality of the handheld IMU.

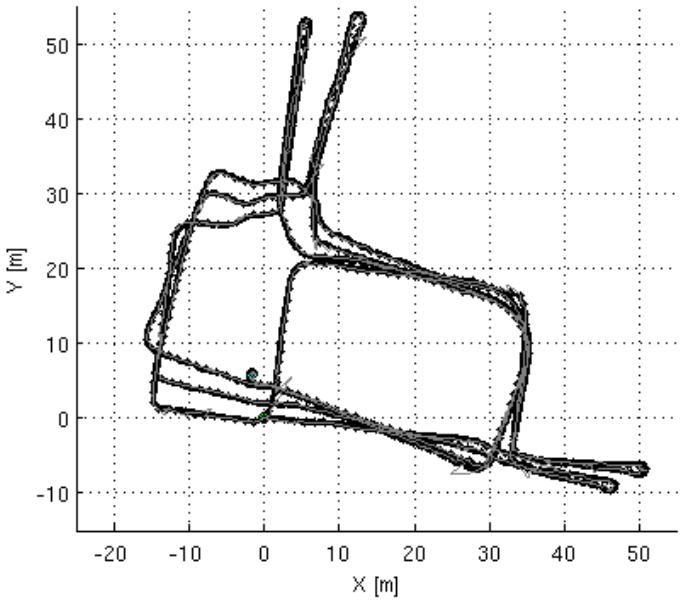

Figure 3: Walker's trajectory as recorded by: (Thick dark line) PDR system output, and (Thin gray line) feedback KF solution for the handheld IMU.

EXPERIMENTAL RESULTS

We conducted a comprehensive series of experiments to assess the performance of our TA system. Each experiment was performed with two types of handheld IMUs, a high quality BAE SiIMU02 [19], and a lower quality MemSense nIMU [20]. The PDR system was the same for all experiments and used a MemSense nIMU.

The experiments were conducted under the following conditions:

The walker was instrumented with a PDR system, which included a boot-mounted nIMU. During the walk the walker held a second IMU in his hand and moved that IMU in some pre-determined ways as detailed below.

In each experiment the walker walked 10 times along a rectangular path. Each experiment lasted about 20 min and the total traveled distance was about 1,000 m (see Figure 4).

The walker started and finished the experiments in the same spot, located half way in a corridor (at X=0, $Y = 0$ in Figure 4).

The walker followed a straight path along the corridors.

Each experiment comprised two walks, one in clockwise (CW) and the other in counter-clockwise (CCW) direction.

In order to gain a better understanding of how TA worked under different conditions, we experimented with different ways of manipulating the handheld IMU during the walks. The following four conditions were tested (one per walk):

1. Handheld IMU pointing forward during the complete walk. We refer to these walks as "normal handling."
2. Handheld IMU oscillating ±45° about the vertical axis, with the IMU changing sides every other step. We refer to these walks as "low frequency handling" (LF).
3. Handheld IMU oscillating ±45° about the vertical axis, with the IMU changing sides on every step. We refer to these walks as "high frequency handling" (HF).
4. Handheld IMU moving randomly without any restriction (side to side, up and down, lateral, tiling, etc.). We refer to these walks as "random handling."

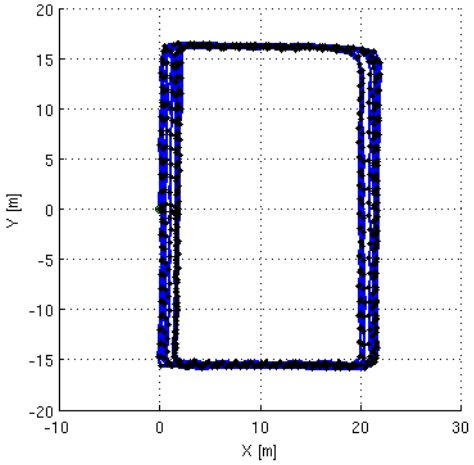

Figure 4: Trajectory of a typical walk as estimated by the PDR system.

The final heading errors were measured as follows. At the beginning of the experiment the walker initialized the heading of the handheld IMU to a fixed and known value by holding the IMU's straight sidewall against a corridor wall. At the end of the experiment the walker did so again, thus assuring that the final heading of the handheld IMU was identical to its initial heading. Since the IMU started and ended with the same heading, any difference between these two measurements can be interpreted as the final heading error. For test purposes the walker realigned the handheld IMU with the corridor wall at the end of each lap (i.e., five times during each walk). This intermediate realignment step does not have any effect on the results but is useful for tuning the KF. In order to verify this claim, one of the four walks in each set of experiments was performed without doing the intermediate realignment and showed similar results.

With each of the two handheld IMUs, we performed four sets of experiments, each set containing eight walks, corresponding to the four different ways of handling the IMU (normal, LF, HF, and random) and two walking directions (CW and CCW). The total number of walks per IMU was 32. Even though our system also corrects positioning errors, we only present the heading errors, which were the main purpose of this work.

In the following illustrations, we show final errors resulting from these walks. In all cases the white vertical bars show the original heading errors without TA, while the black vertical bars show the heading error after applying TA.

High-Grade Handheld IMU (BAE) Results

In this series of experiments, we used a high quality IMU (the BAE SiIMU02) as the handheld IMU. Figures 5 to 8 show the 32 individual results corresponding to these experiments. Figure 9 shows the average heading error when combining all 32 results and **Error! Reference source not found.** tabulates the corresponding numerical values. Because of the high quality of the handheld IMU, the final heading errors are not very large. Nonetheless, the TA algorithm lowered heading errors to less than half of the original errors.

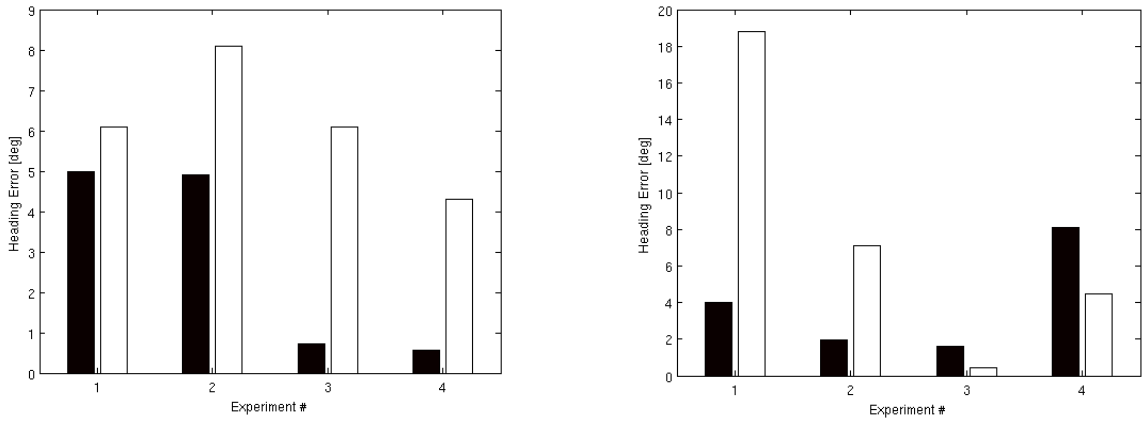

Figure 5: Final heading errors for the normal handling walks. (Left) CW walks; (right) CCW walks. (Black) with TA, (white), without TA.

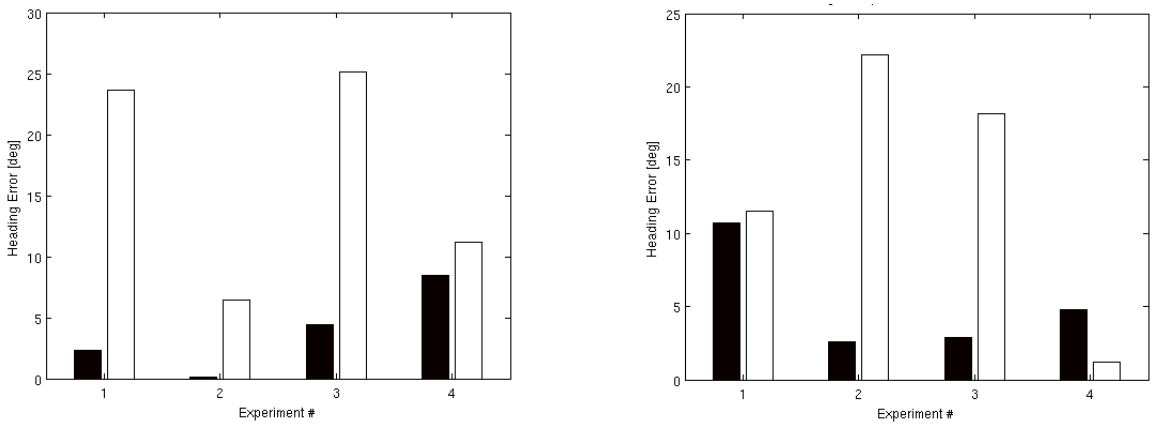

Figure 6: Final heading errors for the high-frequency handling walks. (Left) CW walks; (right) CCW walks. (Black) with TA, (white), without TA.

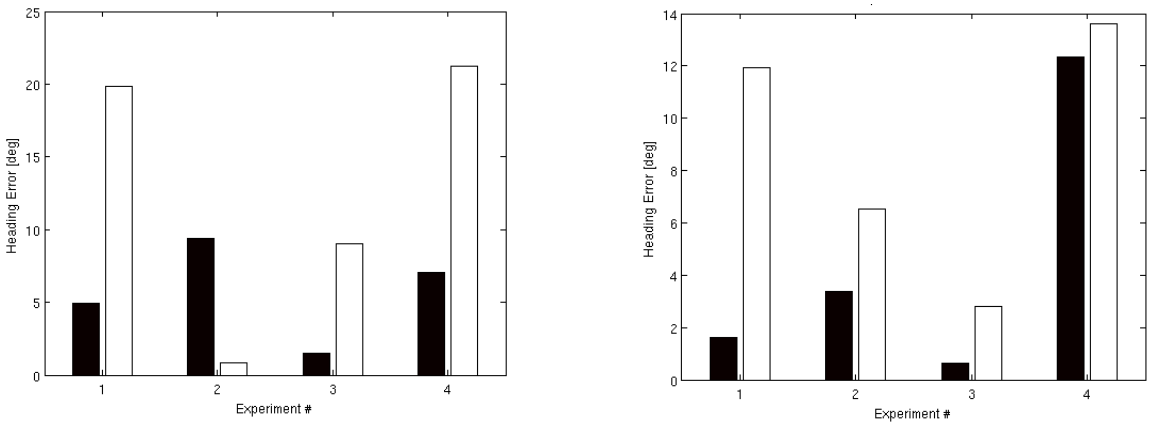

Figure 7: Final heading errors for the low frequency handling walks. (Left) CW walks; (right) CCW walks. (Black) with TA, (white), without TA.

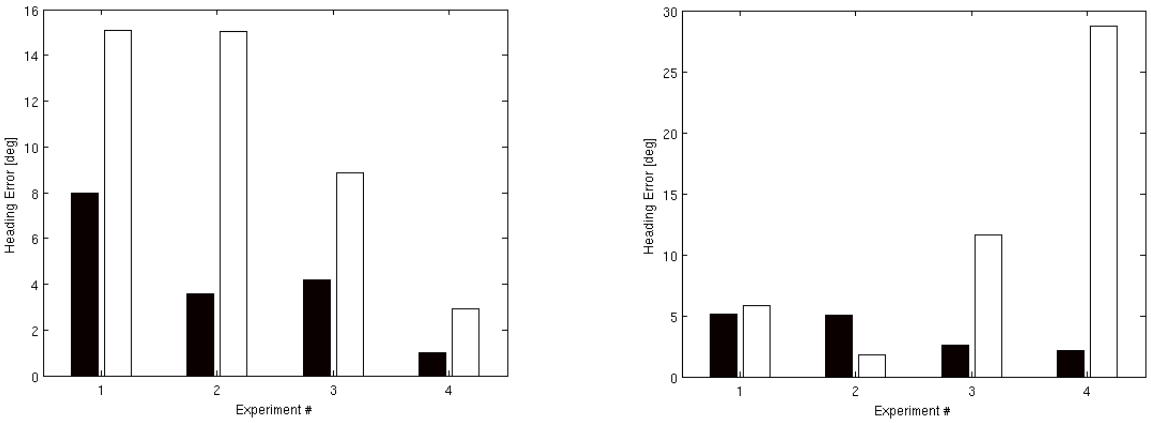

Figure 8: Final heading errors for the random handling walks. (Left) CW walks; (right) CCW walks. (Black) with TA, (white), without TA.

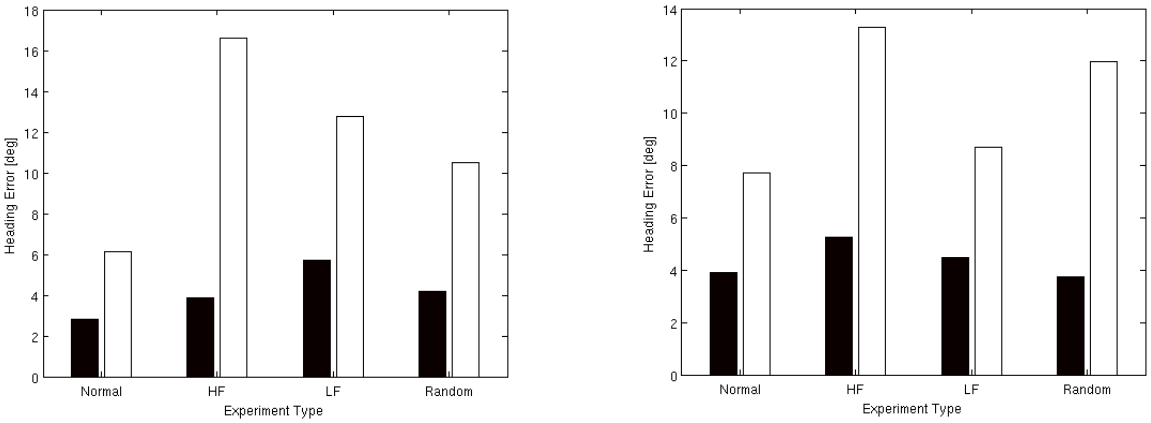

Figure 9: Final average over all walks. (Left) CW walks; (right) CCW walks. (Black) with TA, (white), without TA.

Table I: Average heading errors before and after applying TA for the high-grade handheld IMU (BAE).

Handheld IMU wave pattern	Clockwise walks		Counter-clockwise walks	
	Without TA	With TA	Without TA	With TA
	[deg]	[deg]	[deg]	[deg]
Normal	6.1	2.8	7.7	3.9
High Frequency	16.6	3.9	13.3	5.3
Low Frequency	12.7	5.7	8.7	4.5
Random	10.5	4.2	12.0	3.7
Average	***11.5***	***4.1***	***10.4***	***4.3***

Lower-grade Handheld IMU (Memsense nIMU) Results

In these experiments, we used a lower-quality IMU (the MemSense nIMU) as the handheld IMU. Figures 10 to 13 show the 32 individual results corresponding to these experiments. Figure 14 shows the average heading error when combining all 32 results and Table II tabulates the corresponding numerical values. The final heading errors with the lower-quality handheld IMU are quite significant. Application of the TA algorithm lowered these errors to almost five times the original error.

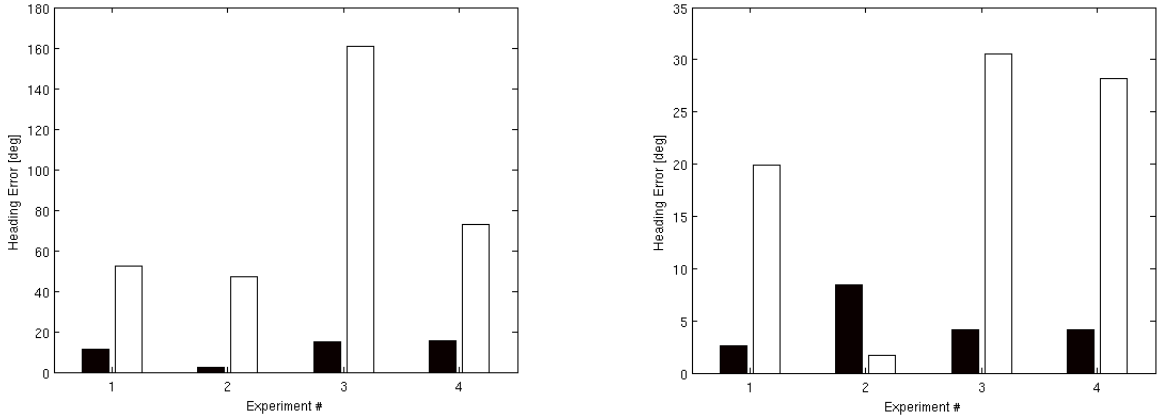

Figure 10: Final heading errors for the normal walks. (Left) CW walks; (right) CCW walks. (Black) with TA, (white), without TA.

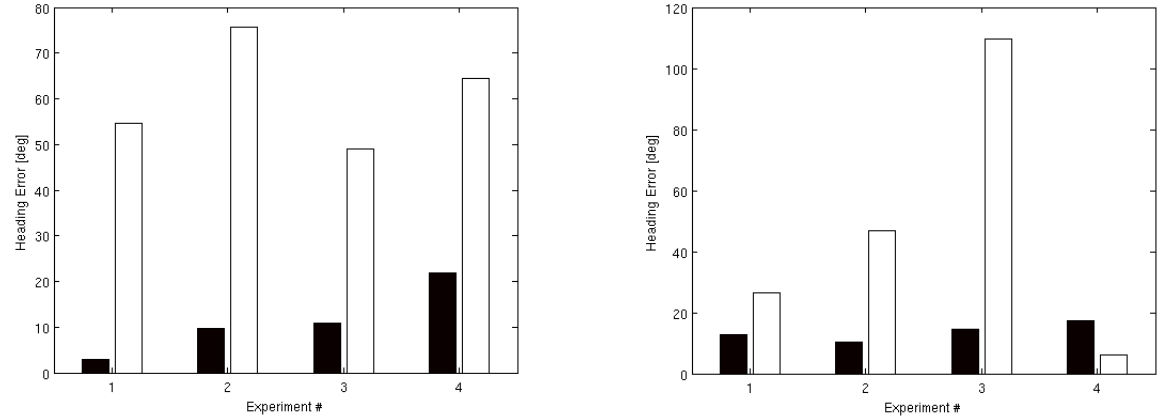

Figure 11: Final heading errors for the high-frequency walks. (Left) CW walks; (right) CCW walks. (Black) with TA, (white), without TA.

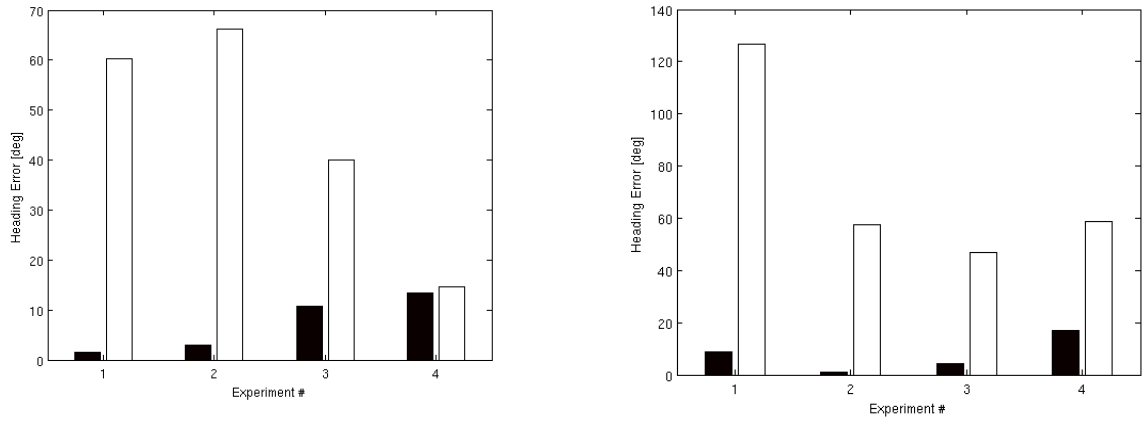

Figure 12: Final heading errors for the low frequency walks. (Left) CW walks; (right) CCW walks. (Black) with TA, (white), without TA.

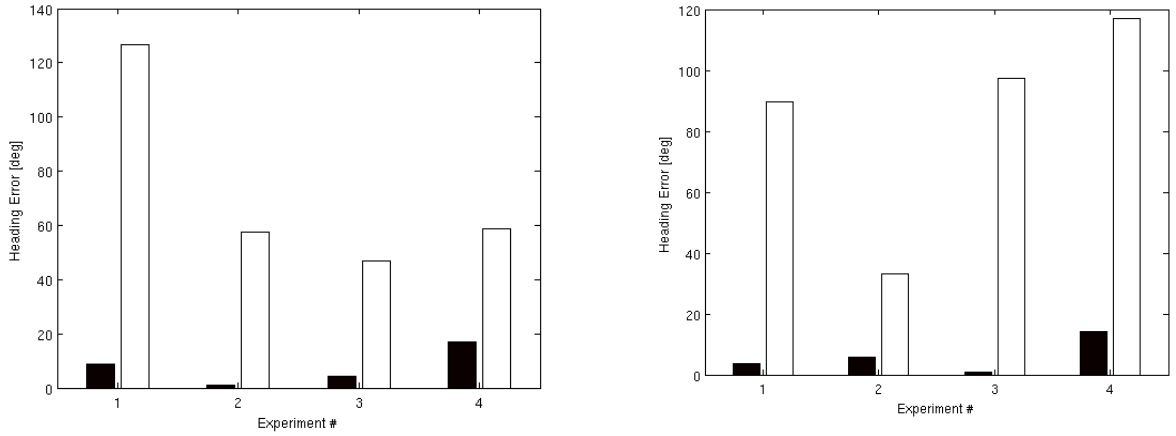

Figure 13: Final heading errors for the random walks. (Left) CW walks; (right) CCW walks. (Black) with TA, (white), without TA.

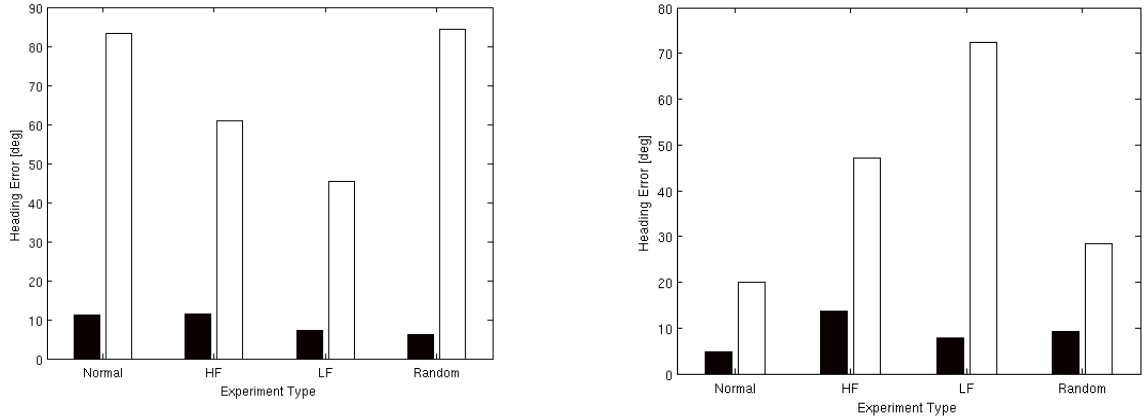

Figure 14: Final average over all walks. (Left) CW walks; (right) CCW walks. (Black) with TA, (white), without TA.

CONCLUSIONS

We successfully implemented and tested a TA algorithm for pedestrian use. The algorithm was developed to correct heading errors for a body-mounted IMU.

When used with a lower-grade IMU, our TA system provides a five-fold reduction in heading errors. With the high-grade IMU, our system provides a more modest two-fold heading error reduction. In practice, head-mounted instruments are unlikely to be equipped with a high-grade IMU since those are significantly heavier and larger (not to mention, costlier) than the MEMs-based lower-grade IMU. Therefore, our results with the lower-grade IMU are more relevant.

Table II: Average heading errors before and after applying TA for the lower-grade handheld IMU (Memsense nIMU)

	Clockwise walks		**Counter-clockwise walks**	
Handheld IMU wave pattern	**Without TA**	**With TA**	**Without TA**	**With TA**
	[deg]	[deg]	[deg]	[deg]
Normal	83.1	11.1	20.1	4.8
High Frequency	61.0	11.4	47.2	13.8
Low Frequency	45.3	7.2	72.4	7.9
Random	84.3	6.2	28.4	9.3
Average	***68.5***	***9.0***	***42.0***	***8.9***

TA does not only reduce the handheld IMU's heading errors, but it is also capable of bounding them indefinitely (relative to the PDR system), that is, the error will not grow with the time. The accuracy of the TA is determined by the characteristics of the IMU and the noise level of the positioning updates (measurement noise). Although it is possible to improve the characteristics of the sensor (i.e. BAE vs Memsense IMU), the measurement noise will remain the same for all cases, setting a lower limit in the accuracy of the system.

Our current implementation of TA treats some errors as a combined noise source. In theory it should be possible to determine the individual bias/error contribution from each gyro by defining the appropriate states in the KF. We tested two KF configurations, feed-forward and feedback, the results presented in this paper used the feed-back configuration.

REFERENCES

[1] PhaseSpace Inc., http://www.phasespace.com
[2] Vicon Motion Systems, http://www.vicon.com
[3] Hofmann, M. and Gavrila, D. M., "Multi-view 3D Human Upper Body Pose Estimation combining Single-frame Recovery, Temporal Integration and Model Adaptation," Proc. of the IEEE Conference on Computer Vision and Pattern Recognition, Miami-FL, (2009)
[4] Organic Motion Inc., http://www.organicmotion.com/
[5] Polhemus, http://www.polhemus.com
[6] Smith, J. R., "Field Mice: Extracting Hand Geometry From Electric Field Measurements," IBM Systems Journal. Vol. 35(3-4), 587-608 (1996).
[7] Ubisense Ltd, http://www.ubisense.net
[8] Maxwell, J. S., "A Low-cost Solution to Motion Tracking Using an Array of Sonar Sensors and an Inertial Measurement Unit," Master of Science Thesis, (2009)
[9] Xsens, http://www.xsens.com
[10] Intersense Inc, http://www.intersense.com
[11] Vlasic, D., Adelsberger, R., Vannucci, G., Barnwell, J., Gross, M., Matusik, E., Popovic, J., "Practical Motion Capture in Everyday Surroundings," in Proc. SIGGRAPH, ACM, (2007)
[12] Joffrion, J. M., Raquet, J. F., "Head Tracking for 3D Audio Using a GPS-Aided MEMS IMU," Proceedings of the National Technical Meeting of The Institute of Navigation, San Diego, CA, 252-259 (2004)
[13] Roll, J., Baillot, Y., Goon, A., "A Survey of tracking technology for virtual environments," in "Fundamentals of wearable computers and augumented reality," CRC Press, 67-110 (2001)
[14] Welch, G. F., "History: The use of the kalman filter for human motion tracking in virtual reality," Journal of Presence: Teleoperators and Virtual Environments. Vol. 18(1), 72-91 (2009)

[15] Ojeda, L., and Borenstein, J., “Non-GPS Navigation for Emergency Responders,” International Joint Topical Meeting: Sharing Solutions for Emergencies and Hazardous Environments. Salt Lake City, UT, (2006).
[16] Borenstein, J, Ojeda, L., and Kwanmuang, S, “Heuristic Reduction of Gyro Drift in a Personal Dead-reckoning System,” Journal of Navigation. Vol. 62(1), 41-58 (2009)
[17] Rogers, R.M., “Weapon IMU transfer alignment using aircraft position from actual flight tests," Position Location and Navigation Symposium, IEEE 1996, 328-335 (1996)
[18] Sun, C., Deng, Z., “Transfer alignment for harmonization of airborne sensors,” Intelligent Control and Automation, WCICA 2008. 7th World Congress on. Vol., 5004-5008 (2008)
[19] BAE Systems, http://www.baesystems.com
[20] Memsense, http://www.memsense.com